^{63}Cu Knight shifts in the superconducting state of $YBa_2Cu_3O_{7-\delta}$ ($T_c = 90$ K)

S. E. Barrett, D. J. Durand, C. H. Pennington, C. P. Slichter,* T. A. Friedmann, J. P. Rice, and D. M. Ginsberg

Department of Physics and Materials Research Laboratory, University of Illinois at Urbana-Champaign, 1110 West Green Street, Urbana, Illinois 61801

(Received 21 July 1989)

The authors have used ^{89}Y NMR to measure the internal magnetic field of a sample of $YBa_2Cu_3O_{7-\delta}$ ($T_c = 90$ K) in the superconducting state to correct for the effects of the Meissner shielding currents. They used this information to separate the magnetic-shift tensor into orbital (chemical-shift) and spin (Knight-shift) contributions. They find that the temperature dependence of the chain Cu Knight shift fits the classic Yosida function of weak-coupling, orbital-*s*-state, spin-singlet BCS theory. For the planes, the Knight shift also requires a spin singlet, but with a strong-coupling Yosida function. The best fit is for an orbital *s* state, but an orbital *d* state is also possible. They find a zero-temperature gap $\Delta(0)$ of $1.76k_BT_c$ for the chains. For the planes, $\Delta(0)$ can range from $1.9k_BT_c$ to $3.1k_BT_c$.

I. INTRODUCTION

It is well known that the nuclear-magnetic-resonance (NMR) Knight shift K^S, can be used to measure the electron-spin susceptibility as a function of temperature in the superconducting state $[\chi^S(T)]$ relative to the normal-state spin susceptibility $[\chi^S(T > T_c)]$ in a superconductor.[1] In close analogy to the theory of superfluid ^{3}He, the functional form of $\chi^S(T)$ can be used to distinguish between different possible types of spin- and orbital-pairing states.[2] It is clearly of great interest to measure $K(T)$ in the superconducting state of the recently discovered high-T_c superconductors in order to calculate $\chi^S(T)$ and derive information about the type of spin-pairing state and the character of the energy gap in these new materials.

We report measurements of the ^{63}Cu Knight shift in $YBa_2Cu_3O_{7-\delta}$ ($T_c = 90$ K) in the superconducting state, using a uniaxially aligned powder sample. Due to demagnetizing currents, the magnetic field inside a type-II superconductor in the superconducting state is not equal to the applied field. Therefore, an essential step in obtaining accurate measurements of $K(T)$ is determining the magnetic field inside the sample. We find that the difference between the fields inside ($B_{\rm int}$) and outside (H_0) the sample are substantial. At 4.2 K, $B_{\rm int}$ is 0.05% lower than H_0 when $\mathbf{H}_0 \| \mathbf{c}$, and 0.02% lower when $\mathbf{H}_0 \perp \mathbf{c}$. We obtain high precision and reliability by using the ^{89}Y resonance frequency to measure the internal field of the sample directly. This is possible because the ^{89}Y Knight shift is known to be very small on the scale of the Cu shifts,[3–6] as we discuss below. The measurements are difficult because the ^{89}Y spin-lattice relaxation times are long and the gyromagnetic ratio, γ_Y, is small, but we have found means to carry them out with high precision.

We find that the Cu(1) (chain) $\chi^S(T)$ follows the conventional *weak-coupling* Bardeen-Cooper-Schrieffer (BCS) form for an *s*-state singlet (the Yosida function[7]) with the low-temperature gap given by $2\Delta(T=0) = 3.52k_BT_c$, where T_c is the superconducting transition temperature. The Cu(2) (plane) $\chi^S(T)$, on the other hand, can be fit by an *s*-wave or *d*-wave spin-singlet *strong-coupling* Yosida function assuming energy gaps which are larger than the weak-coupling value.

Takigawa *et al.* were the first to measure the ^{63}Cu Knight shifts in the superconducting state $YBa_2Cu_3O_{7-\delta}$.[8] They corrected for the demagnetizing effects mentioned above by measuring the resonant frequency and magnetization M versus the applied field at 7 K. From these measurements they deduced the relationship between the internal field correction and M at this temperature. They then measured M at each new temperature, and used this relationship to calculate the corresponding internal field correction. They point out that there is uncertainty in their diamagnetic correction and warn that one feature of their corrected data is probably spurious. We have made the determination of the ^{63}Cu Knight shifts versus temperature, $K(T)$, reported here because knowledge of $K(T)$ is of fundamental importance and because our use of the ^{89}Y NMR to make the internal field correction is expected to be very reliable. Our results for the Cu Knight shifts differ substantially from those of Takigawa *et al.* in both the zero-temperature values and temperature dependences.

II. EXPERIMENT

Our $YBa_2Cu_3O_{7-\delta}$ sample was prepared by thoroughly mixing and grinding $BaCO_3$, Y_2O_3, and CuO powders (99.999% pure) in a dry nitrogen atmosphere and reacting the mixture in air at 950 °C for 24 h, with two intermediate grindings. The powder was then placed on a platinum sheet and treated in a stream of pure oxygen at 900 °C for 24 h and slowly cooled to room temperature at a rate of 12 °C/h. The Meissner effect is shown as the inset of Fig. 1. The procedure used to align the crystallites

was essentially that of Farrell *et al.*[9] A sample holder was devised which allowed the sample to have a well-defined orientation with respect to the field. The $YBa_2Cu_3O_{7-\delta}$ sample powder was passed through a No. 400 mesh screen, so that the crystallites used were all smaller than 38 μm in diameter. Next, 1.98 g of the resulting $YBa_2Cu_3O_{7-\delta}$ powder was stirred into epoxy (Stycast 1266) with an approximate packing fraction of 0.1 by volume. This mixture was placed in the sample holder and cured in a 8.1-T field. The *c* axes were well aligned along the field direction, as confirmed by the sharp features in the ^{63}Cu NMR spectrum. Figure 1 shows the normal-state NMR spectrum taken at 100 K with $\mathbf{H}_0\|\mathbf{c}$ and $\mathbf{H}_0\perp\mathbf{c}$ with the transition frequencies observed in our earlier studies of an oriented single crystal indicated for comparison.[10]

In making this aligned powder sample, we found that passing the powder through the mesh resulted in more complete alignment, possibly because small particles of powder are more likely to be single crystallites, or because small particles rotate in the epoxy with less resistance under the torque applied by the magnetic field during the cure.

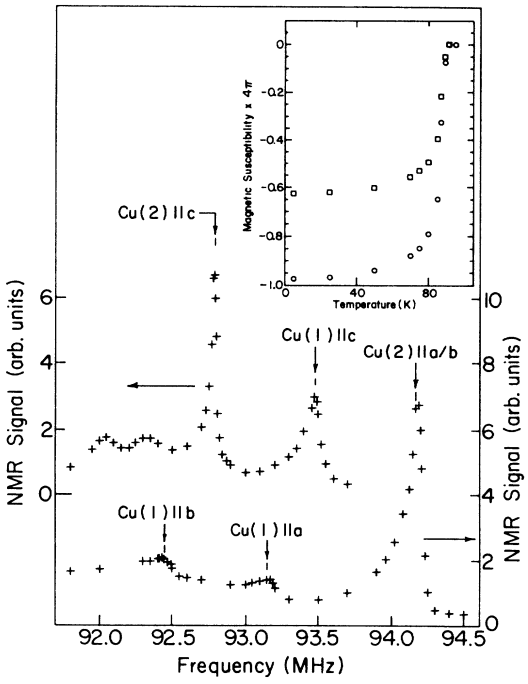

FIG. 1. Inset: the magnetization of the sample powder (see text) vs temperature in 16 Oe for field cooled (open squares), and zero-field cooled (open circles) showing a sharp superconducting transition at 90 K and complete magnetic shielding. Main figure: the upper curve is the ^{63}Cu NMR line shape of the aligned sample at 100 K with $\mathbf{H}_0\|\mathbf{c}$. The lower curve is the line shape with $\mathbf{H}_0\perp\mathbf{c}$. The arrows above both curves indicate the positions of the single-crystal lines measured previously (Ref. 10). The two broad (unlabeled) peaks at the low-frequency end of the upper curve are the ^{63}Cu(1) $\pm\frac{3}{2}$, $\pm\frac{1}{2}$ transitions.

A key aspect of this experiment is the use of the ^{89}Y NMR to measure the field inside the sample. Measurement of the ^{89}Y resonance line is difficult both because γ_Y is low and because at low temperatures the spin-lattice relaxation time is long. We have used two techniques which make it possible to observe the ^{89}Y NMR at low temperatures.

The first is to use a Carr-Purcell-Meiboom-Gill sequence to collect data.[11] We have previously used this method to speed data collection of Nb in $NbSe_3$ (Ref. 12) and ^{17}O in CO on surfaces.[13] In an ordinary spin echo (two pulses plus one echo), the magnetization is destroyed. One must then wait for a time comparable to the spin-lattice relaxation time to be able to record a second echo. In a Carr-Purcell sequence, one repeatedly refocuses the nuclear magnetization observing multiple echoes before one must refresh the nuclear magnetization. The pulse sequence we use starts with a 90_x pulse, followed at time τ by a 180_y. The echo that forms at τ after the 180_y pulse is recorded. One then repeats the wait time of τ, the 180_y pulse, and records the echo formed τ after the 180_y pulse. Thus, the sequence to record *n* echoes is

$$90_x-(\tau-180_y-\tau-\text{ record echo})_n\ . \tag{1}$$

In our case we found we could go up to $n=16$ in the superconducting state. When we add the echoes together we enhance the signal-to-noise ratio by

$$\frac{S}{N}=\left[\frac{S}{N}\right]_0\frac{1}{\sqrt{n}}\left[\frac{1-r^n}{1-r}\right], \tag{2}$$

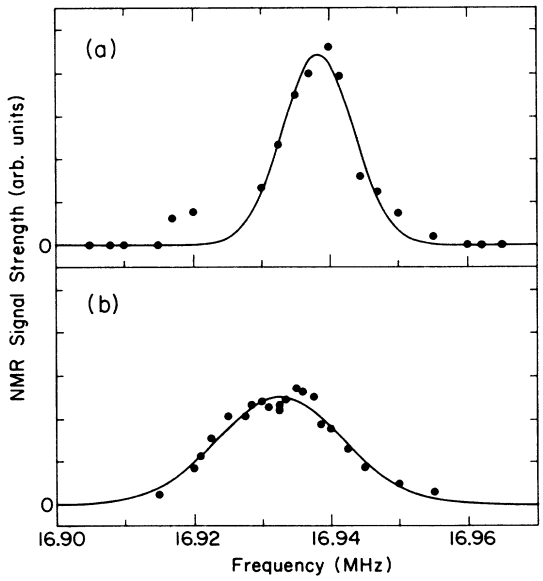

FIG. 2. The ^{89}Y NMR line shape of the aligned sample at 4.2 K for (a) $\mathbf{H}_0\perp\mathbf{c}$ and (b) $\mathbf{H}_0\|\mathbf{c}$. The solid lines are the Gaussians found by the least-squares method where the center frequency, amplitude, and width are adjusted to optimize the fit to the data.

where $(S/N)_0$ is the signal-to-noise ratio of the first echo, n is the number of echoes, and r is the ratio of consecutive echo amplitudes in the Carr-Purcell train. In this case, $(S/N) \approx 2.5(S/N)_0$, or equivalently, with Carr-Purcell we can get a given (S/N) in about one-sixth the time it would take with single-spin echoes.

The second technique used is also called for because the low-temperature ^{89}Y spin-lattice relaxation time is so long. In the superconducting state, the ^{89}Y line is too broad relative to the strength of the alternating field, H_1, to be reliably measured by Fourier transform of the spin echo. Thus, we must record the ^{89}Y line point by point. By using a sufficiently small H_1, one can excite one region of the line without perturbing other regions. We thus divide the ^{89}Y line into three frequency intervals. We collect an echo in region 1, then in region 2, lastly in region 3. By the time one finishes the third point, the magnetization has recovered near the first point. Now one repeats the cycle for new frequencies first in region 1, then in region 2, finally in region 3. This approach makes efficient use of the time one has to wait for the spins to become polarized along H_0. Figure 2 shows the ^{89}Y line shapes at 4.2 K for $\mathbf{H}_0 \| \mathbf{c}$ and $\mathbf{H}_- \perp \mathbf{c}$.

III. DATA ANALYSIS

The features seen in the 100-K ^{63}Cu line shape (Fig. 1) can also be seen in the superconducting state line shapes. Figure 3(a) [Fig. 3(b)] shows the ^{63}Cu line shape at 4.2 K for $\mathbf{H}_0 \| \mathbf{c}$ ($\mathbf{H}_0 \perp \mathbf{c}$).

Our procedure for determining $K(T)$ is as follows: At each temperature and field orientation, the resonance frequency of each site [Cu(1) and Cu(2)] is calculated by exact diagonalization of the Hamiltonian using the electric field gradient (EFG), the magnitude of the magnetic field inside the sample, and an initial guess for the value of K. The calculated frequency is then compared to that measured. This procedure is repeated, adjusting K at each iteration, until the calculated and measured frequencies agree. Explicitly, at each temperature we need four quantities to determine K: (1) and (2) the two independent parameters of the EFG tensor, (3) the internal magnetic field, and (4) the measured resonance frequency. We now consider each of these in turn.

We have assumed that the EFG tensor retains its 100-K anistropy but that the magnitude of each component has a small, linear temperature dependence as indicated by the temperature dependence of the nuclear quadruple resonance frequency.[14]

We use the ^{89}Y NMR line to give the magnitude of the internal field. At any temperature, the ^{89}Y resonant frequency, f_Y, will be given by

$$f_Y = [1 + K_Y(T)] \frac{\gamma_Y}{2\pi} B_{\text{int}} , \tag{3}$$

where $K_Y(T)$ is the ^{89}Y magnetic shift and γ_Y is the gyromagnetic ratio by ^{89}Y. Uncertainties in f_Y and K_Y will both lead to an uncertainty in B_{int}. Figure 4 shows

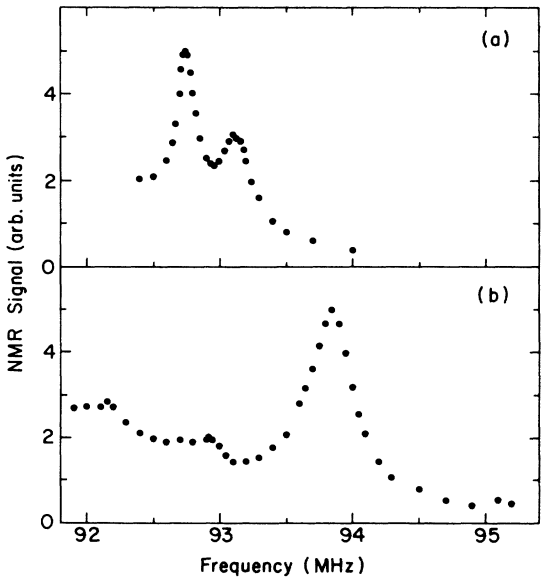

FIG. 3. The ^{63}Cu line shape at 4.2 K with (a) $\mathbf{H}_0 \| \mathbf{c}$ and (b) $\mathbf{H}_0 \perp \mathbf{c}$.

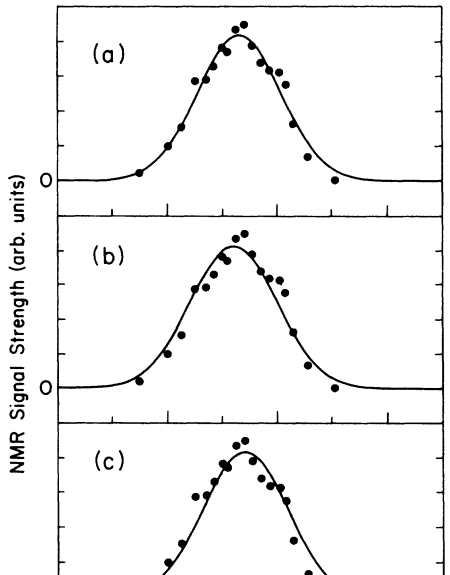

FIG. 4. The ^{89}Y line at 20 K with $\mathbf{H}_0 \| \mathbf{c}$. The data points, which are the integral of the sum of Carr-Purcell-Meiboom-Gill spin echoes vs the oscillator frequency, are the same in all three figures. The solid line in (a) is the Gaussian found by the method of least squares where the center frequency, amplitude, and width are adjusted to optimize the fit to the data. The solid line in (b) [(c)] is the Gaussian found by the method of least squares where the amplitude and width are adjusted to optimize the fit to the data given that the center frequency is offset by -1 kHz ($+1$ kHz) from the optimal value. The fits in (b) and (c) are the limits of what can be called a reasonable fit to the data and we take these to be the limits of our uncertainty in frequency.

that we can measure f_Y to within about $\pm 0.006\%$. Figure 4(a) shows the data (solid circles) and the Gaussian found by the method of least squares adjusting the amplitude width, and center frequency; Figs. 4(b) and 4(c) show the same data with Gaussians found by the method of least squares adjusting the amplitude and width given that the center frequency is offset from the optimal value by -1 and $+1$ kHz, respectively. It is clear that the true center frequency of the data is between these limits.

Before we proceed with the data analysis, it is interesting to consider the shape of the ^{89}Y line. In these experiments, the sample is in the mixed state and H_0 is well above H_{c1}. We estimate that the fluxoids are on the order of 200 Å apart.

It is well known that the fluxoids through a single, flat, uniform piece of type-II superconductor in the mixed state with H_0 perpendicular to the flat face can form a regular two-dimensional (2D) pattern. This pattern, or lattice of fluxoids, leads to a characteristic field distribution throughout the sample.[1] One might have expected to see such structure in our ^{89}Y lines. We do not. As can be seen in Figs. 2 and 4, our ^{89}Y lines are Gaussians. It is important to keep in mind, however, that in our sample we also expect two random sources of broadening to be important. First, there is a spread in demagnetizing factors for various particle shapes. Second, a particle can experience additional randomly oriented fields due to the magnetic moments of neighboring particles. One can show that these effects may be comparable to the broadening due to fluxoids. At any rate, we conclude from the fact that our ^{89}Y NMR lines are Gaussian, that either the random sources of broadening completely obscure any characteristic line shape due to a particular flux lattice, or the fluxoids are not in a regular array to begin with.

We also need to know what value of K_Y to use at each temperature. We know K_Y quite well in the normal state. We have measured it to be -150 ppm (-95 ppm) relative to YCl_3 when $\mathbf{H}_0\|\mathbf{c}$ ($\mathbf{H}_0\perp\mathbf{c}$). These values agree with those previously measured by other groups.[3-6] The decomposition of the normal-state shift into orbital (chemical-shift) and hyperfine (Knight-shift) components is the subject of work by several groups. Balakrishnan *et al.*[5] show that typical chemical shifts of ^{89}Y in various insulating oxides is 120–230 ppm relative to YCl_3, making the Knight shift in $YBa_2Cu_3O_7$ $-250--350$ ppm. Alloul *et al.*[6] plot $\sqrt{1/T_1T}$ versus shift for $YBa_2Cu_3O_{6+x}$ for x between 0.41 and 1. Extrapolating their data to $\sqrt{1/T_1T}=0$ gives a Knight shift between -300 and -400 ppm ($-0.03--0.04\%$). Throughout the rest of this paper we will take the value of K_Y ($T=100$ K) to be ($-0.030\pm0.005\%$).

Because we expect the Knight-shift part of K_Y will be reduced in the superconducting state, we must assume a functional form of the ^{89}Y Knight shift versus temperature. The ^{89}Y nuclei in the normal state appear to be in an environment very much like that of a metal with nearly independent (weakly interacting) conduction electrons. The ^{89}Y spin-lattice relaxation rate ($1/T_1$) is very accurately proportional to the temperature.[3,5,6] Therefore, we will assume the Y Knight shift is given in the superconducting state by the standard Yosida function.[7]

We point out that the uncertainty in K_Y at any temperature is small (about $\pm 0.005\%$). It is also important to note that our assumed functional form of $K_Y(T)$ is flat from 0 to about 30 K. It is very unlikely that our choice will have any effect on the temperature dependence of $K_{Cu}(T)$ at low temperatures.

We next need to accurately measure the ^{63}Cu resonant frequencies at low temperatures. The low-temperature ^{63}Cu lines are broadened by the same distribution in B_{int} discussed above in relation to the ^{89}Y line. Therefore, we scale the ^{89}Y line breadth in frequency by the ratio of the gyromagnetic ratios (γ_{Cu}/γ_Y) to get the ^{63}Cu Gaussian broadening function in frequency. We then convolute this with a particular feature in the observed 100-K ^{63}Cu line shape, and determine the frequency shift needed to superpose that broadened line on the data of the superconducting phase. Figure 5 shows such a fit at 4.2 K for the chain [Cu(1)] and plane [Cu(2)] nuclei with $\mathbf{H}_0\|\mathbf{c}$. With the relative shift between the superconducting state and the $T=100$-K lines, and our single-crystal measurements of the frequencies of the various lines in the normal state,[10] we can get precise values for the frequencies of the low-temperature lines

In this procedure we discovered an extra broadening of the Cu(2) line at low temperature when $\mathbf{H}_0\perp\mathbf{c}$. Figure 6 shows the comparison of the 100-K line broadened by the amount implied by the ^{89}Y line (dashed line) with the measured Cu(2) (open circles) at 4.2 K, with $\mathbf{H}_0\perp\mathbf{c}$. The experimental line is seen to be several times broader than the line predicted by scaling the ^{89}Y line.

Assuming that the extra broadening does not lead to a net shift in the Cu(2) line, we proceed with the data analysis by convoluting an additional broadening with

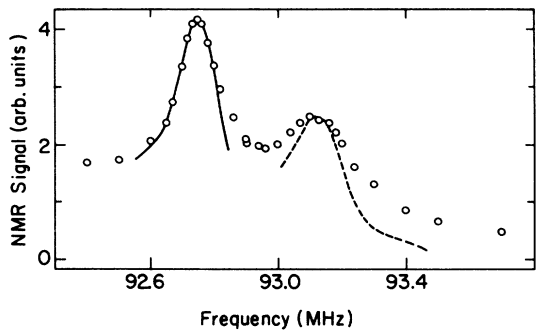

FIG. 5. A demonstration of how the low-temperature lines are fit with the broadened 100-K data. The points are the measured line shape at 4.2 K with $\mathbf{H}_0\|\mathbf{c}$. The solid and dashed lines are the broadened and shifted 100-K line shapes of the appropriate peaks. The broadening used is Gaussian with a width implied by the measured ^{89}Y linewidth. Because this broadening accounts for most (or all) of the low-temperature linewidth, the low-temperature broadening represents a distribution of magnetic fields throughout the sample.

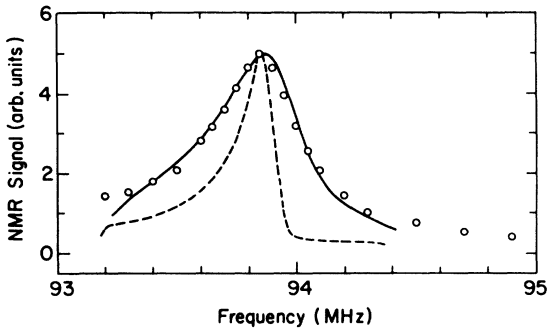

FIg. 6. The points are the ^{63}Cu(2) line shape at 4.2 K for $\mathbf{H}_0 \perp \mathbf{c}$. The dashed curve is an attempt to fit the low-temperature line shape with the broadened and shifted 100-K line as described in Fig. 5. The solid curve is a fit to the 4.2-K data using the broadened and shifted 100-K line with an additional Lorentzian broadening (see text).

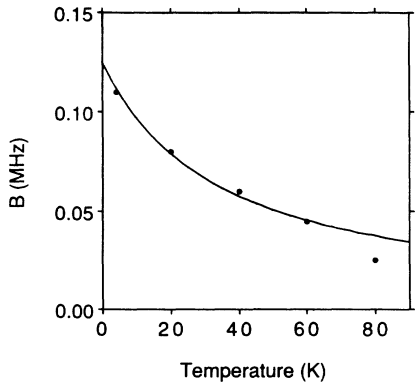

FIG. 8. The solid points are the extra broadening, over and above that implied by the measured ^{89}Y linewidth, needed to fit the low-temperature Cu(2) central line with $\mathbf{H}_0 \perp \mathbf{c}$ (see text). The solid line is the functional form of the temperature dependence given in the text.

the already broadened 100-K ^{63}Cu line (see the solid line in Fig. 6) and then determining the relative frequency shift. The total magnetic shift $K(T)$ determined by this procedure is shown in Fig. 7. We will give a detailed discussion in Sec. IV of the data in Fig. 7.

We investigated several possible sources of the additional broadening of the Cu(2) line in the superconducting state with $\mathbf{H}_0 \perp \mathbf{c}$. By comparing the ^{63}Cu and ^{65}Cu central transitions at 4.2 K, we have shown that the extra line breadth arises from magnetic and not electric quadrupole effects. Measurement of the ^{63}Cu satellite line ruled out the possibility that either $(K_{aa}-K_{bb})$ or $(\nu_{aa}-\nu_{bb})$ had become large enough at low temperatures to account for the extra broadening. We also measured the Cu(2) $\mathbf{H}_0 \perp \mathbf{c}$ line again, using a recovery time between successive echoes (T_{rep}) of 10 sec. The new T_{rep} was 33 times longer than the original T_{rep}. This new line shape had the same shape and width as the original line shape, and we get about the same size signal for the planes in both the $\mathbf{H}_0 \| \mathbf{c}$ and the $\mathbf{H}_0 \perp \mathbf{c}$ orientations. These two results showed that we had not missed a long T_1 component of the signal, ruling out another possible explanation of the measured line breadth.

We obtained the best fit to the data when we convoluted a Lorentzian of half-width B with the 100-K data broadened by the ^{89}Y Gaussian. The extra broadening necessary to fit the Cu(2) data follows a Néel temperature

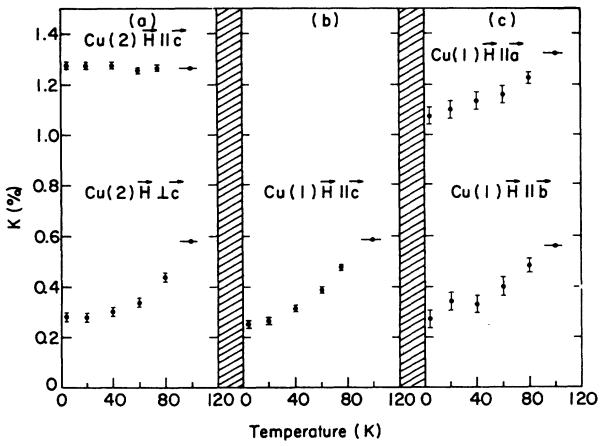

FIG. 7. The total magnetic shift as a function of temperature for (a) Cu(2) with (upper) $\mathbf{H}_0 \| \mathbf{c}$ and with (lower) $\mathbf{H}_0 \perp \mathbf{c}$, (b) Cu(1) with $\mathbf{H}_0 \| \mathbf{c}$, (c) Cu(1) with (upper) $\mathbf{H}_0 \| \mathbf{a}$ and with (lower) $\mathbf{H}_0 \| \mathbf{b}$.

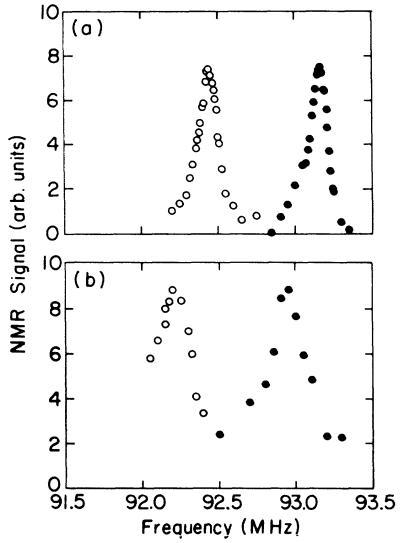

FIG. 9. The ^{63}Cu(1) resonance lines with $\mathbf{H}_0 \| \mathbf{a}$ (higher frequency) and $\mathbf{H}_0 \| \mathbf{b}$ (lower frequency) in the multi-single-crystal sample described in the text at (a) 100 K and (b) 4.2 K. In this sample the field is either along the a or b axis of any given untwinned region in each of the crystals. The fact that the separation between these peaks is approximately the same at both these temperatures is consistent with our finding (from measurements made on the uniaxially aligned sample) that the Cu(1) Knight shift is roughly isotropic.

dependence of the form

$$B(T)=\frac{4.29\ \text{K MHz}}{T+34.29\ \text{K}} \tag{4}$$

quite well between 4.2 and 60 K, as is shown in Fig. 8.

In an effort to improve the precision of data when $\mathbf{H}_0\perp\mathbf{c}$, where the chain line shapes are restricted powder patterns, we made a sample consisting of some 50 tiny single crystals of $YBa_2Cu_3O_{7-\delta}$. The c axes of the crystals were aligned by placing their broad face on a flat plexiglass surface, then the a-b axes were oriented by rotating each crystal under a cross-polarized light microscope (see Ref. 10). With this array of single crystals we could observe the Cu resonances in both the normal and superconducting states. Data for the chains with H_0 along a and b at 100 and 4.2 K are shown in Fig. 9. These measurements are consistent with our finding in the powder sample that $[K_a(100)-K_{aa}(4.2)]$ and $[K_{bb}(100)-K_{bb}(4.2)]$ are very nearly the same. This single-crystal sample also confirms the presence of the anomalous broadening of the Cu(2), $\mathbf{H}_0\perp\mathbf{c}$ line.

IV. THE SHIFTS: GENERAL ASPECTS

In the original BCS theory, the superconducting wave function involved pairing of electrons into states which are spin singlets with orbital-angular-momentum zero (s-state, spin-singlet pairing). But pairings are possible involving spin triplets, as well as other orbital angular momentum states (spin singlets involve even-l orbital angular momentum, spin triplets involve odd-l orbital angular momentum). These matters are treated extensively in the review article of Leggett on Fermi liquids.[2] There it is shown that one expects to find that the spin susceptibility, χ^S in the superconducting state is either unaffected by the transition

$$\chi^S=\chi_n\ , \tag{5}$$

where χ_n is the susceptibility in the normal state, or

$$\chi^S=Y_l(T)\chi_n\ , \tag{6}$$

where $Y_l(T)$ is some function which depends on the angular momentum l involved in the pairing. [Ordinarily Eq. (6) holds for all three components of the susceptibility, or Eq. (5) holds for two components and Eq. (6) for the third. The so-called planar state is the only example we know of where Eq. (5) holds for one component and Eq. (6) holds for the other two.] An example of $Y_l(T)$ is the $l=0$ function for spin singlets named after Yosida.[7] The temperature dependence of $Y_l(T)$ as T approaches zero depends on l and the pairing state. For a system with no nodes, $Y_l(T)$ has zero slope at $T=0$. For a d wave, $Y_l(T)$ varies linearly with T as $T\rightarrow 0$. These matters are discussed by Monien and Pines.[15]

The results of our data analysis are shown in Fig. 7 as plots of total magnetic shift versus temperature. The magnetic shifts $K_{\alpha\alpha}(T)$ shown in Fig. 7 are made up of two parts:

$$K_{\alpha\alpha}(T)=K^L_{\alpha\alpha}+K^S_{\alpha\alpha}(T)\ , \tag{7}$$

where K^L is the orbital (chemical) shift, and $K^S(T)$ is the spin (Knight) shift. In a BCS picture with a singlet-pairing state, one expects that pairing will lead to a vanishing spin susceptibility at $T=0$, and consequently $K^S(T=0)=0$. This has been demonstrated experimentally in Al by Hammond *et al.*[16] The measurements of the Knight shift of mercury in the superconducting state by Reif[17] and the subsequent theoretical description by Anderson[18] demonstrate, however, that this picture is modified in the presence of strong spin-orbit coupling which occurs for heavy elements such as mercury and tin. The simple BCS picture is expected to hold for Cu, where spin-orbit coupling is less strong. We will assume $K^S_{\alpha\alpha}(T=0)=0$, and investigate the consequences for $K^L_{\alpha\alpha}$. The temperature-independent chemical shift ($K^L_{\alpha\alpha}$) is then all the remains of the total magnetic shift $K(T)$ at absolute zero. Thus, $K^L_{\alpha\alpha}=K(4.2\ \text{K})$. From the data shown in Fig. 7 we have determined the shift tensor $K_{\alpha\alpha}$ ($\alpha=a,b,c$) at 4.2 K and $\Delta K_{\alpha\alpha}$, the difference between the shift tensors at 100 and 4.2 K. These are given in Table I.

As discussed by Pennington *et al.*[10] in the approximation that the Cu^{++} is an ion with a hole in its d shell and a permanent electron spin moment, the orbital contribution (chemical shift) is given by

$$K^L_{\alpha\alpha}=2\beta^2\left[\sum_n \frac{(0|L_\alpha|n)(n|L_\alpha/r^3|0)}{E_n-E_0}+\text{c.c.}\right] \tag{8a}$$

$$=4\beta^2\left\langle\frac{1}{r^3}\right\rangle\sum_n\frac{|(0|L_\alpha|n)|^2}{E_n-E_0} \tag{8b}$$

$$=2\left\langle\frac{1}{r^3}\right\rangle\chi^L_{\alpha\alpha}\ , \tag{8c}$$

where $\alpha=a,b,c$ are the conventional crystal axes (which are also the principal axes of the orbital shift) and $\chi^L_{\alpha\alpha}$ is orbital contribution to the magnetic susceptibility. If the d-shell hole extends onto neighboring atoms, one must go back to (8a) to see exactly how to evaluate (8b).

We can evaluate Eq. (8) for both the Cu(2) and the Cu(1) sites. We define $(x,y,z)=(a,b,c)$. Consider first the Cu(2) site. The crystal field is axially symmetric about the z axis. For a hole in the x^2-y^2 d shell, and defining the energy of the that state as zero, one finds

TABLE I. The total magnetic shift K and the change in K between $T=100$ and 4.2 K, ΔK.

	$K(T=100\ \text{K})$[a]	$K(T=4.2\ \text{K})$[b]	ΔK[b]
Cu(1) $\mathbf{H}_0\|\|\mathbf{c}$	0.588	0.25±0.01	0.33±0.01
Cu(1) $\mathbf{H}_0\|\|\mathbf{a}$	1.323	1.08±0.04	0.25±0.04
Cu(1) $\mathbf{H}_0\|\|\mathbf{b}$	0.561	0.27±0.04	0.29±0.04
Cu(2) $\mathbf{H}_0\|\|\mathbf{c}$	1.267	1.28±0.01	−0.01±0.01
Cu(2) $\mathbf{H}_0\perp\mathbf{c}$	0.580	0.28±0.02	0.30±0.02

[a]We do not include limits of error on the normal-state values of K because the procedure for finding the superconducting-state values uses the 100-K values as given.

[b]These are the results assuming the ^{89}Y Knight shift is −300 ppm.

$$K_{zz}^L = 16\beta^2 \left\langle \frac{1}{r^3} \right\rangle \frac{1}{E_{xy}} ,$$
$$K_{xx}^L = 4\beta^2 \left\langle \frac{1}{r^3} \right\rangle \frac{1}{E_{yz}} \quad (9)$$
$$= K_{yy}^L \text{ for axial symmetry} .$$

For axial symmetry, one expects $E_{yz} \geq E_{xy}$. The calculation for the Cu(1) site is analogous, except the crystal field is now axially symmetric about the x axis (a axis). Thus we find

$$K_{cc}^L \geq 4K_{aa}^L = 4K_{bb}^L \text{ for the planes [Cu(2)]} ,$$
$$K_{aa}^L \geq 4K_{bb}^l = 4K_{cc}^L \text{ for the chains [Cu(1)]} , \quad (10)$$

where the equality corresponds to the case that the excited d states xy and yz (yz, xz) are degenerate for the Cu(2) [Cu(1)]. This ionic permanent moment model describes very well the behavior of the ^{63}Cu atoms in the normal state.[10]

From Table I we see that

$$K_{cc}^L = 4.54 K_{aa}^L \quad \left[\frac{E_{yz}}{E_{xy}} = \frac{E_{xz}}{E_{xy}} = 1.14 \right]$$

for the Cu(2) nuclei, and

$$K_{aa}^L = 4.24 K_{cc}^L = 3.94 K_{bb}^L \quad \left[\frac{E_{xz}}{E_{yz}} = 0.99, \ \frac{E_{xy}}{E_{yz}} = 1.07 \right]$$

for the Cu(1) nuclei. The fact that these ratios agree with Eq. (10) strongly supports our assumption that $K^S(T=0)=0$. Consequently, we may now interpret $\Delta K_{\alpha\alpha}$, which is the difference between the total shift at 100 and 4.2 K, as the Knight shift at 100 K, K^S(100 K) (see Table I). We now turn to an analysis of these data, first for the Cu(1) and then the Cu(2) sites.

V. THE CHAINS

We see that to a good approximation K^S(100 K) is isotropic for the Cu(1) site ($\approx 0.29 \pm 0.04$ %). The Knight shift with $\mathbf{H}_0 \| \mathbf{a}$ appears to be somewhat smaller than that with $\mathbf{H}_0 \| \mathbf{b}$; however, these are the most difficult lines to measure at low temperature and thus there is uncertainty in their shift values. The single-crystal data shown in Fig. 9 are consistent with K^S(100 K) being, to a good approximation, isotropic.

Pennington *et al.* measured the spin-lattice relaxation rate coefficients, with the field along each axis at 100 K, and found $(W_1)_\alpha$ of $(1.1 \pm 0.1, 0.9 \pm 0.1, 0.8 \pm 0.1$ msec$^{-1})$ where $\alpha = a, b, c$ which are likewise, to a good approximation, isotropic.[10] Various workers have measured the spin-lattice relaxation time of the Cu(1) nuclei.[14,19] We have measured it in an unoriented powder of our $YBa_2Cu_3O_{7-\delta}$ material using nuclear quadrupole resonance (NQR). At each temperature we measured the relaxation curve using the inversion recovery method. Figure 10 shows the relaxation curves at two temperatures. Plotted is $\log_{10}[S(\infty) - S(t)]$ versus t, where $S(t)$ is the signal observed in a spin echo applied at time t after the inversion pulse. The data are seen to fit a single exponential (the expected form) for over two decades of signal strength. The time constant of this decay is $(T_1)_{NQR}$. Figure 11 shows $(1/T_1)_{NQR}$ versus T. We see that $(1/T_1)_{NQR}$ is proportional to T with very great precision from 100 to 150 K, and that even at 180 K the deviation is only about 5%. For higher temperatures, $(1/T_1)_{NQR}$ deviates from linearity with T. Evidently, at higher temperatures another relaxation mechanism becomes important.

We want to compare the linear component of $(1/T_1)_{NQR}$ with the magnitude of the Knight shift. The Korringa relation,[20] for nuclei relaxed by electrons in a conduction band, is

$$(T_1)_z T (K^S)^2 = \left[\frac{\hbar}{4\pi k_B} \right] \frac{\gamma_e^2}{\gamma_n^2} B , \quad (11)$$

where K^S is the Knight shift, k_B is the Boltzmann constant, and B is a factor introduced by Pines to take into

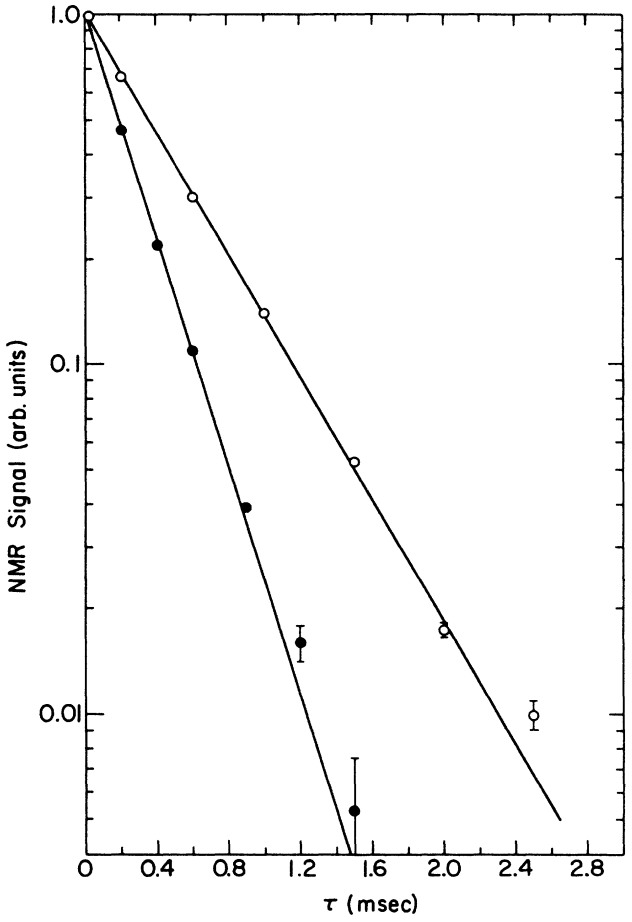

FIG. 10. The spin-lattice relaxation curves at $T = 103$ K (open circles), and $T = 160$ K (solid circles) measured by inversion recovery. Plotted is $[S(\infty) - S(t)]/S(\infty)$, where S is the size of the spin echo and t is the time between a 180° inversion pulse and the first pulse of the 90°-τ-180° spin-echo pulse sequence. The expected form of the decay is a single exponential such as is shown by the solid lines, the slope of which is $1/T_1$.

account many-body effects.[20] If spin-$\frac{3}{2}$ systems such as ^{63}Cu and ^{65}Cu had no electric quadrupole splittings so that we have solely Zeeman splittings, the spin-lattice relaxation would be exponential with a time constant we denote as $(T_1)_z$ such that $(1/T_1)_z=\frac{2}{3}W_1$, so that from our previous relaxation data for the Cu(1) site,[10] $(1/T_1)_z=0.62$ msec^{-1}, or $(T_1)_z=1.61$ msec. Equation (11) is satisfied with $K=0.29\%$, $(T_1)_z=1.61$ msec, and $B=0.36$ ($B=1.0$ for noninteracting conduction electrons or holes). A B of 0.36 would imply some antiferromagnetic interaction between the conduction electrons, but is essentially in the weak-coupling limit.

The most precise chain data, $K_{cc}^S(T)$, fit a standard weak-coupling BCS Yosida function extremely well, as is shown in Fig. 12. The Yosida function was calculated assuming s-wave pairing, and it reflects the decrease in the conduction electron density of states at the Fermi level as a gap is opened.[7] The curves for $K_{aa}^S(T)$ and $K_{bb}^S(T)$ are less clear, but it is important to keep in mind that there is more uncertainty in those measurements. The crystallites in our sample are aligned along their c axes, their a and b axes are randomly distributed in the plane perpendicular to the c axes. As a result, the resonance frequencies corresponding to the cases $\mathbf{H}_0\|\mathbf{a}$ and $\mathbf{H}_0\|\mathbf{b}$ for the Cu(1) site are most difficult to locate with a powder pattern (see Fig. 1). The data for $\mathbf{H}_0\perp\mathbf{c}$ may also be fit by a weak-coupling, s-wave Yosida function but with much larger scatter.

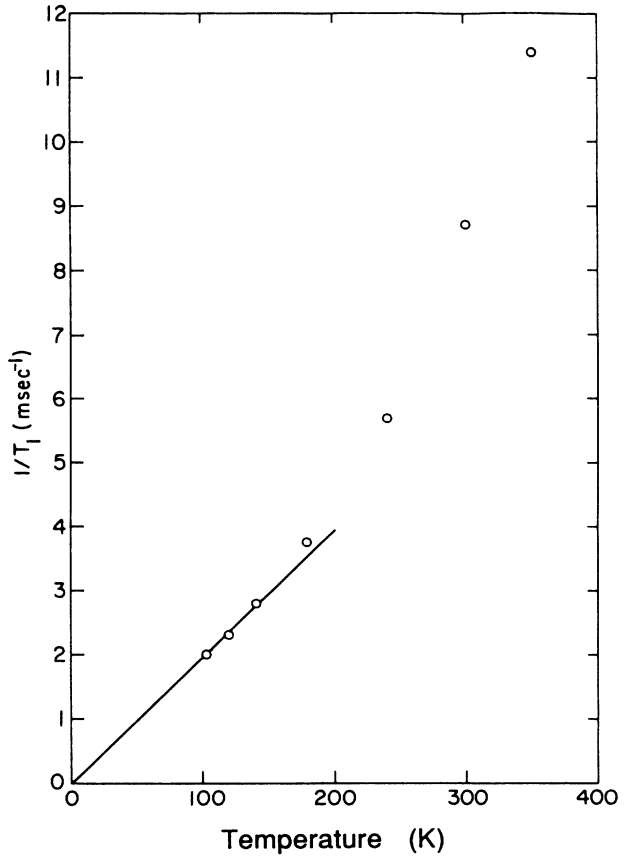

FIG. 11. The spin-lattice relaxation rate $(1/T_1)$ (determined as described in Fig. 10) vs temperature T. The fact that the rate is accurately proportional to T from 100 to 150 K is an indication that the relaxation is due to interaction with electrons in a conduction band. The deviation from linearity for $T>150$ K probably represents another relaxation mechanism.

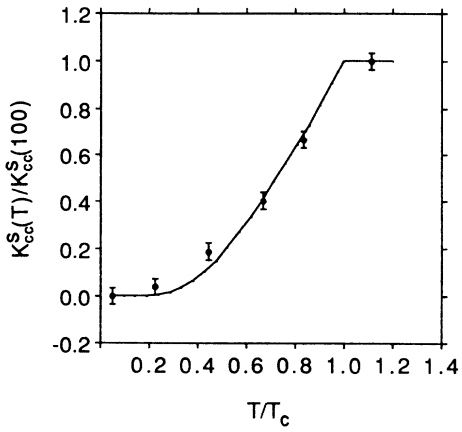

FIG. 12. The normalized Knight shift of the Cu(1) nuclei. The points are the data determined as described in the text. The solid line is the Yosida function as calculated for BCS, weak-coupling, spin-singlet, $l=0$ pairing (Ref. 7).

In summary, the Cu(1) data have the following characteristics: (1) K^S and W_1 at 100 K are essentially isotropic, (2) $T_1T=$const from 100 to about 160 K, (3) the Knight shift and T_1T values satisfy the Korringa relation essentially in the weak-interaction limit, and (4) $K(T)$ in the superconducting state is fit by the weak-coupling Yosida function.

In our earlier paper we postulated that Cu(1) T_1 arose from transferred hyperfine coupling to a hole in the conduction band formed by the chain and bridge oxygen atoms. This coupling would explain all four of the experimental facts listed above provided that the oxygen hole band is a weakly interacting conduction band, or Fermi liquid, and that the Cu(1) shift and relaxation are determined by the coupling to that band.

Since the chemical shift and EFG tensors of the Cu(1) atoms correspond to a single hole in the Cu(1) $3d_{y^2-z^2}$ state, we still assume that Cu(1) atoms have a net electron spin of $\frac{1}{2}$. The fact that this net spin does not contribute to the Knight shift or the Cu(1) nuclear T_1 requires that the electron spin be rapidly scattered, perhaps by the O hole, and that its spin susceptibility must be very small. This implies that the temperature dependence of the chain Knight shift $K^S(T)$ is due to the temperature dependence of the $\chi^h(T)$ alone, since the shift arises from chain holes.

One possible model for the transferred hyperfine coupling involves states at the top of the oxygen-hole band. These states are made up of O(1) and O(4) (chain and bridge) $2p_\sigma$ orbitals, whose symmetry relative to the Cu(1) sites is nearly the same as that of the Cu(1) (y^2-z^2) orbitals. Such states are shown in Fig. 13. Because the bridge oxygens are closer to the Cu(1) atom than the chain oxygens are, the overlap of the O $2p_\sigma$ orbitals with

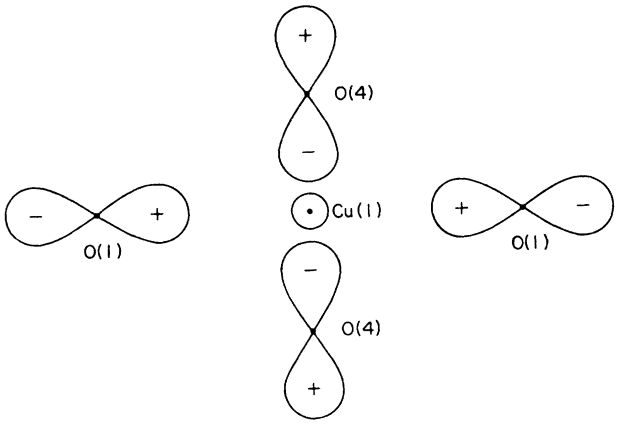

FIG. 13. A schematic illustration of how the $3p$ orbitals of the four neighboring oxygen atoms can mix with the $4s$ orbital of the Cu(1) atom leading to the transferred hyperfine coupling described in the text.

the Cu(1) atom is larger for the bridge oxygens than for the chain oxygens. Thus, the oxygen-band wave function acting at the Cu(1) nucleus contains some Cu $4s$ wave function which leads to the isotropic nature of W_1 and $K(T)$. If this model is correct, the Knight shift for the Cu(1), K^S, is proportional to χ^h, the susceptibility of the O holes.

The above analysis does not depend on the detailed model describing the chain oxygen holes. We now explore a particular model in which we describe the oxygen holes by a one-dimensional conduction band of width B_W. In such a model, the Pauli susceptibility of the holes is

$$\chi^h = 2\beta^2 \rho_1(E_F) , \tag{12}$$

where β is the Bohr magneton, and $\rho_1(E_F)$ the density of states of one spin orientation at the Fermi energy E_F.

In a one-dimensional band, the density of states has an integrable infinity at the top and bottom of the band. If one represents the qualitative k dependence of the energy by

$$E(k_y) = \frac{B_W}{2}(1 - \cos k_y b_0) , \tag{13}$$

where b_0 is the lattice period, with the band edges being $k_y = 0$ and $k_y b_0 = \pm\pi$,

$$\rho_1(E(k)) = 2/(\pi B_W \sin k_y b_0) \tag{14}$$

normalized per Cu(1) atom. The minimum value of $\rho(E)$ is thus $(2/\pi B_W)$, the maximum value is infinite.

The Knight shift is

$$K^S = \frac{8\pi}{3}|\psi(0)|^2_{E_F}\chi^h = \frac{16\pi}{3}|\psi(0)|^2_{E_F}\beta^2\rho_1(E_F) . \tag{15}$$

For a free Cu atom $\frac{16}{3}\pi|\psi(0)|^2_{4S} = 0.45\times 10^{+27}$ (Ref. 21) corresponding to

$$\tfrac{8}{3}\pi|\psi(0)|^2_{4S}(2\beta) = 4172 \text{ kG} .$$

If $|\psi(0)|^2_{E_F} = \alpha|\psi(0)|^2_{4S}$, then for $\alpha = 0.1$, $\rho_1(E_F) = 1.25$ eV^{-1}, for $\alpha = 0.3$, $\rho_1(E_F) = 0.42$ eV^{-1}. Since the chain Cu is Cu^{2+} whereas $|\psi(0)|^2_{4S}$ corresponds to a neutral Cu, the use of $|\psi(0)|^2_{4S}$ will underestimate the hyperfine coupling arising from a given degree of overlap with O $2p$ wave functions. Mila and Rice[22] estimate the charge effect gives a factor of 2 enchancement.

Even the largest value of B_W which results from this simple model is smaller than that in a typical metal. However, we do not yet have a firm theoretical understanding of the nature of the oxygen holes in this material.

VI. THE PLANES

The data for the Cu(2) site have several distinctive features. The most obvious is the absolute flatness of the $K_{cc}(T)$ data from 100 to 4.2 K. In addition, $K_{aa}(T)$ [or $K_{bb}(T)$] has a much steeper slope around $T = T_c$ than the weak-coupling s-wave Yosida function. In the weak-coupling limit, the Yosida functions for higher angular-momentum pairing states lie above the Yosida function for an s-wave paring state.[23] Thus, the simplest BCS model, which worked well for the chains, is not appropriate for the planes. We present a simple model which is consistent with the data, but may not be the only possibility.

We will employ the analysis developed by Monien, Pines, and Slichter (MPS).[24] It represents a generalization of our earlier analysis by including an extra term in the Hamiltonian, an extra term in the shift, and using data from the antiferromagnetic state of reduced oxygen crystals. We first consider the hyperfine coupling to Cu(2) spins. Like Pennington *et al.*, MPS treat the Cu(2) as having a single hole in the $3d_{x^2-y^2}$ state, an electron spin of $\frac{1}{2}$, and a permanent electron-spin magnetic moment. The electron spin couples to its own nucleus through the hyperfine tensor $A_{\alpha\alpha}$. Following Mila and Rice,[22] MPS also include a coupling between the nuclear spin and the electron spin of the nearest-neighbor Cu(2) atoms through an isotropic transferred hyperfine coupling of strength B_1. Thus, the Hamiltonian becomes

$$\hat{H} = \sum_{k,\alpha}\left[I_{k,\alpha}A_{\alpha\alpha}S_{k,\alpha} + B_1\sum_j (I_{k,\alpha}S_{j,\alpha})\right] \quad (\alpha = x,y,z) , \tag{16}$$

where I is the nuclear-spin operator, S is the electron-spin operator, and $\sum_j$ is the sum over the four nearest neighbors of the nucleus k. Mila and Rice also include a transferred hyperfine coupling to the chain Cu. We neglect that term for simplicity. Expressing the coupling as a magnetic field acting on nucleus k with components h_α, we then have

$$h_\alpha = -\frac{1}{\gamma_n\hbar}\left[A_{\alpha\alpha}S_{k\alpha} + B_1\sum_j S_{j\alpha}\right] \tag{17}$$

and the time-average mean-square field

$$\overline{h_\alpha^2}=\frac{1}{4(\gamma_n\hbar)^2}(A_{\alpha\alpha}^2+4B_1^2) \tag{18}$$

if we can set correlations such as $\langle S_{k\alpha}S_{j\alpha}\rangle=0$ for $k\neq j$, where the brackets $\langle\ \rangle$ signify thermal average of the expectation value. Utilizing the relations of Pennington *et al.*[10] for the spin-lattice relaxation rate $(W_1)_\alpha$:

$$(W_1)_i=\tfrac{3}{2}(\gamma_n)^2(\overline{h_j^2}+\overline{h_k^2})\tau_0\ , \tag{19}$$

where $i,j,k=a,b,c$ and cyclic permutations and the measured $(W_1)_\alpha$'s, we find that

$$\frac{\overline{h_c^2}}{\overline{h_a^2}}=7.8\pm1.0$$

or (20)

$$\left[\frac{\overline{h_c^2}}{\overline{h_a^2}}\right]^{1/2}=2.8\pm0.2$$

which puts a constraint on the values of $A_{\alpha\alpha}$ and B_1. Thus, we can write, using Eq. (17), the electron-spin contribution to the Cu(2) Knight shift

$$K_{\alpha\alpha,\mathrm{Cu}}^S=\frac{(A_{\alpha\alpha}+4B_1)}{\gamma_e\gamma_n\hbar^2}\chi_{\alpha\alpha}^S\ , \tag{21}$$

where $\chi_{\alpha\alpha}^S$ is the Cu(2) electron-spin susceptibility. Takigawa *et al.*[8] postulated that, in addition, the Cu(2) had a positive Knight-shift contribution from oxygen holes. The MPS analysis follows this approach, adding an isotropic $B^h\chi^h$ term to the Cu(2) Knight shift. We know such a shift occurs for the Cu(1) (see Sec. V) from admixture of Cu 4*s* states. Examination of the bridge O(4) wave function shows it should also induce Cu 4s density at the Cu(2) nucleus. The total spin contribution to the shift is then

$$K_{\alpha\alpha}^S=\frac{(A_{\alpha\alpha}+4B_1)\chi_{\alpha\alpha}^S+B^h\chi^h}{\gamma_e\gamma_n\hbar^2}\ , \tag{22}$$

where χ^h is the spin susceptibility of the oxygen band and the B^h is the hyperfine coupling constant. We have neglected the contribution of this term to spin-lattice relaxation at this point, but discuss it later in this paper.

One naturally might wonder if there is also a coupling to holes on the oxygen of the Cu(2) plane. Simple symmetry arguments appear to rule out a coupling of such holes to Cu(2) *s* states at least for holes near the top of the O band. As one gets away from the top, such terms are permitted. Another possibility arises from the necessity that the planar O hole functions be orthogonalized to the Cu(2) x^2-y^2 hole state. The orthogonalization will effectively mix some Cu(2) x^2-y^2 function into the O band. In the analysis below we neglect such effects because usually effects involving Cu 4*s* states dominate when they are present. Such effects are already included in Eq. (22). An alternative would be to assume that effects involving Cu 4*s* states are absent and that the term $B^h\chi^h$ we encounter below should be replaced by an anisotropic term proportional to χ_p^h, the spin susceptibility of the planar holes.

Examination of the Cu(2) data shows (1) that K_{cc} is within experimental error independent of T, but (2) $K_{aa}=K_{bb}$ is strongly temperature dependent. The question naturally arises whether the fact that $K_{cc}(T)$ is independent of T is the result of its components each being temperature independent or the result of an accidental cancellation of two temperature-dependent terms. This is important because if each component is temperature independent, then χ_{cc}^S would be temperature independent and this would have important consequences for the nature of the pairing state.

We first consider the possibility that $B^h\chi^h=0$, perhaps because either χ^h or B^h is small. If this is true, then $(A_{cc}+4B_1)\chi_{cc}^S$ must be independent of temperature. One way this can happen is if

$$(A_{cc}+4B_1)=0\ , \tag{23a}$$

which means

$$\frac{A_{cc}}{4B_1}=-1\ . \tag{23b}$$

But from (18) and (20) we know that

$$\frac{\overline{h_c^2}}{\overline{h_a^2}}=\frac{4(A_{cc}/4B_1)^2+1}{4(A_{aa}/4B_1)^2+1}=(7.8\pm1.0)\ . \tag{24}$$

If $(A_{cc}/4B_1)=-1$, this gives us

$$\frac{\overline{h_c^2}}{\overline{h_a^2}}=\frac{5}{4(A_{aa}/4B_1)^2+1}\ , \tag{25}$$

which has a maximum value of five (when A_{aa} vanishes), and thus conflicts with the experimental ratio of (20). Hence, we can rule out $A_{cc}+4B_1=0$.

According to Monien and Pines, the other possibility, that χ_{cc}^S is independent of temperature, but $\chi_{aa}^S=\chi_{bb}^S$ is temperature dependent would, in the BCS theory, correspond to the so-called planar state. At $T=0$ for this state $\chi_{aa}(0)=\frac{2}{3}\chi_{aa}(T_c)=\chi_{bb}(0)$. Examination of Fig. 7 shows that this would require that $K_{aa}^L(0)$ and $K_{bb}^L(0)$ be *negative* for the Cu(2)'s, a circumstance ruled out by Eq. (8).

We therefore conclude $B^h\chi^h\neq0$. We have then

$$K_{cc}^S=\frac{(A_{cc}+4B_1)\chi_{cc}^S+B^h\chi^h}{\gamma_e\gamma_n\hbar^2}\ , \tag{26a}$$

$$K_{aa}^S=\frac{(A_{aa}+4B_1)\chi_{aa}^S+B^h\chi^h}{\gamma_e\gamma_n\hbar^2}\ . \tag{26b}$$

The data indicate that both $\chi_{aa}^S(T)$ and $\chi_{bb}^S(T)$ obey Eq. (6). The general arguments given by Leggett (coupled with the rejection of the planar state as a possibility) require $\chi_{cc}^S(T)$ to obey Eq. (6) as well.[2] Thus, all three components of $\chi_{\alpha\alpha}^S(T)$ have the same temperature dependence.

For simplicity, we take $\chi^S(100)$ to be isotropic. If this is not the case, the values for the coupling constants would change, but our results, which depend on the prod-

ucts of the coupling constants and $\chi^S(T)$, do not.

We can eliminate $B^h\chi^h$ in Eq. (26) by subtracting K_{cc}^S from K_{aa}^S

$$K_{aa}^S(T)-K_{cc}^S(T)=(A_{aa}-A_{cc})\chi^S(T) \tag{27a}$$

or

$$K_{aa}(T)-K_{cc}(T)=(K_{aa}^L-K_{cc}^L)+(A_{aa}-A_{cc})\chi^S(T)\ . \tag{27b}$$

We have subtracted the $K_{cc}(T)$ data from the $K_{aa}(T)$ data and normalized the result (taking the data at 4.2 K as being the zero). The result is plotted in Fig. 14. Figures 14(a) and 14(b) show the same data with different theoretical curves which we will explain below. It is important to note that the ^{89}Y Knight shift is eliminated from this plot, since it occurs equally in K_{aa} and K_{cc}.

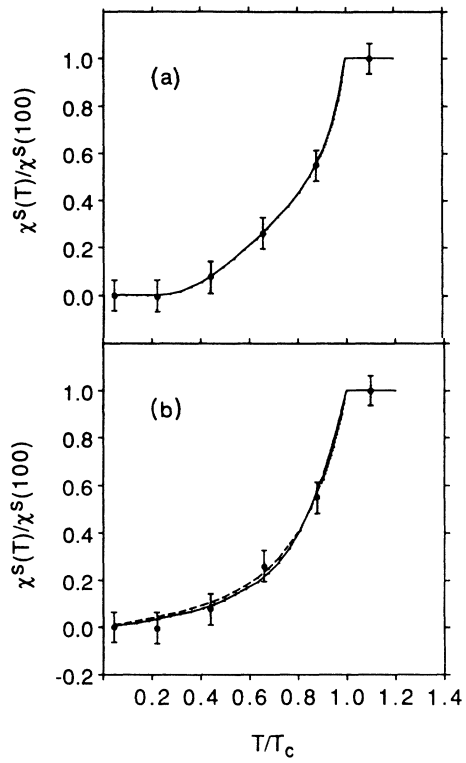

FIG. 14. The points are the difference between $K_{aa}(T)$ and $K_{cc}(T)$ for the Cu(2) atoms. These points should represent the contribution to the Knight shift from the Cu(2) electron moments. The two solid lines in (a) overlap. The first is a strong-coupling Yosida function derived by Monien assuming an s-wave pairing state with a $2\Delta(T=0)=3.8k_BT_c$ value for the zero-temperature gap. The second is a strong-coupling Yosida function derived by Monien assuming an anisotropic s-wave pairing state with a $2\Delta(T=0)_{max}=4.3k_BT_c$ value for the zero-temperature gap. The solid line in (b) is a strong-coupling Yosida function derived by Monien assuming a d-wave pairing state with a $2\Delta(T=0)_{max}=29.34k_BT_c$ value for the zero-temperature gap. The dashed line in (b) is a strong-coupling Yosida function derived by Monien assuming a d-wave plus higher-l-term pairing state with a $2\Delta(T=0)_{max}=6.26k_BT_c$ value for the zero-temperature gap.

The standard weak-coupling Yosida function which works so well for the Cu(1) $K(T)$ lies well above these data.

In thinking about these data, it is helpful to keep in mind a simple picture of the Fermi surface. We do not assert it is precise, but it provides a useful means of considering one theoretical limit. Several groups have calculated the band structure in the limit that the Cu atoms are treated in a band picture.[25] However, we find that in the normal state, the Cu atoms behave as though they have permanent moments. Then the oxygen holes may be thought of in a simple manner as consisting of a two-dimensional band associated with the plane oxygens, and a one-dimensional band associated with the chain and bridge oxygens. The former give approximately cylindrical Fermi surfaces with the cylinder axis perpendicular to the k_x,k_y plane. The latter give planar Fermi surfaces normal to the k_y direction.

In conjunction with our colleagues Monien and Pines, we have explored various means of fitting these data. The Yosida function $Y(T)$ which describes both the Knight shift and the spin susceptibility is given by Leggett as

$$Y(T)=\int_{-\infty}^{\infty}N(E)\left[-\frac{\partial f}{\partial E}\right]dE\ , \tag{28}$$

where $N(E)$ is the superconducting density of states. It varies with temperature because the gap is temperature dependent. One can use Eq. (28) therefore to calculate $Y(T)$ for various assumptions about the gap and its temperature dependence. Monien and Pines[15] found that a strong-coupling version of the s-state singlet gave a good fit. [See Fig. 14(a).]

Monien and Pines have analyzed spin-lattice relaxation times as well as Knight shifts. It is well known that there is an enhancement of the spin-lattice relaxation rate immediately below T_c for s-state BCS superconductors.[26] The size of the enhancement depends on the energy level width and the anisotropy of the energy gap.[23] Accordingly, Monien and Pines consider various energy gap anisotropies by making the energy gap for the planes depend on the angle ϕ about the axis of the cylindrical portion of the Fermi surface. They consider s-wave spin-singlet pairing with and without gap anisotropy, and d-wave spin-singlet pairing both with a single d wave (gap proportional to $\cos\phi$) and a d wave containing higher harmonics. The different assumptions have substantial effects on the spin-lattice relaxation times because of their effect on the enhancement. For the Knight shifts, the two s-wave cases are indistinguishable graphically, and the two d-wave cases are barely distinguishable. Indeed, their difference is much smaller than the experimental errors of our data.

In Fig. 14(a) the solid curve results from the s-wave calculation, and in Fig. 14(b) the solid curve results from the d-wave calculation. For the s wave $\Delta(0)$ (the energy gap at $T=0$ K) is $1.90k_BT_c$ for the isotropic gap. For the s-wave anisotropic gap $\Delta(0)_{max}=2.16k_BT_c$.

For the single d wave $\Delta(0)_{max}=14.67k_BT_c$ whereas for their function containing higher harmonics $\Delta(0)_{max}$

$=3.13k_BT_c$.

The best looking fits are for the *s*-wave states, although we cannot rule out the *d*-wave fits. The isotropic *d*-wave fit has a very large value for the gap and is thus more suspect than the anisotropic *d* wave. Whichever *l*-pairing fit we use, the gap needed is larger than the BCS value. We note, however, that the values obtained for these gaps are quite sensitive to small changes in the data.

VII. THE NORMAL STATE

In our earlier work[10] we showed that the Cu(2)'s could be understood in terms of a model in which the Cu(2) had a single hole in the x^2-y^2 orbit and a net electron spin $\frac{1}{2}$. At that time we did not include the possibility of a transferred hyperfine interaction B_1 nor an explicit hole contribution $B^h\chi^h$ in Eqs. (23) or (26). Now that we have a more complete set of Cu(2) electronic parameters, we can make more theoretical progress. In addition to Eqs. (8) and (20)–(22), we utilize the expressions of Bleaney *et al.*[27]

$$\frac{A_{cc}}{\gamma_e\gamma_n\hbar^2}=\left\langle\frac{1}{r^3}\right\rangle\left[-\kappa-\frac{4}{7}-\lambda\left[\frac{6}{7E_{xz}}+\frac{8}{E_{xy}}\right]\right],$$
$$\frac{A_{aa}}{\gamma_e\gamma_n\hbar^2}=\left\langle\frac{1}{r^3}\right\rangle\left[-\kappa+\frac{2}{7}-\frac{11}{7}\frac{\lambda}{E_{xz}}\right]. \quad (29)$$

Monien, Pines, and Slichter[24] have extended our model to include B_1 and $B^h\chi^h$ as well as a relationship from NMR in the antiferromagnetic state of the O_6 1:2:3 compound (in kG)

$$\frac{(A_{aa}-4B_1)2\langle S_z\rangle}{\gamma_n\hbar}=-160 \quad (30)$$

which uses the measured antiferromagnetic resonance frequency.[28] Using the measured values of shift at 4.2 and 100 K, and the measured $(W_1)_\alpha$'s, we can obtain many parameters of the normal state. If we assume the reasonable values for three parameters $\kappa=0.28$, $\lambda=-0.088$ eV $=-710$ cm^{-1}, $2\langle S_z\rangle=0.6$, then we can use an MPS-type analysis supplemented with an iterative procedure leading to self-consistent values. We can calculate for the Cu(2) all of the following quantities:

$A_{cc}=-427$ kG ,

$A_{aa}=38$ kG ,

$B_1=76$ kG ,

$\langle 1/r^3\rangle=6.0$ a.u. ,

$E_{xy}=2.72$ eV, $E_{xz}=3.08$ eV ,

$\chi^S=12.2\times10^{-29}$,

$\chi^L_{cc}=15.8\times10^{-29}$ emu/Cu(2) ,

$\chi^L_{aa}=3.5\times10^{-29}$,

$\chi_{\rm tot}=20.0\times10^{-29}$,

$\tau_0=1.1\times10^{-15}$ sec .

These values are typical of Cu^{2+} ions. $\chi_{\rm tot}$ is the powder average of the total susceptibility per Cu(2) atom and may be compared with the value 27×10^{-29} emu/Cu deduced from the measured susceptibility by Junod, Benzinge, and Muller.[29] The fact that we get such a good account of so many features of the data lends strong support to the picture of Cu(2) in the normal state as being close to the permanent moment limit.

Recently Yasuoka *et al.*[30] have reported NQR relaxation studies of the Cu(2) nuclei in a number of high-T_c and related metallic oxides. They conclude that in a number of them the spin-lattice relaxation rate $(1/T_1)_{\rm NQR}$ has a component which is linear in temperature above about 200 K. In $YBa_2Cu_3O_{6.91}$ they get, for this component, $(1/T_1)_{\rm NQR}=4.5T$ (sec^{-1}). The term $B^h\chi^h$ in our analysis implies an associated relaxation mechanism. Since $B^h\chi^h$ is from the oxygen-hole band, its contribution to the relaxation will be linear in T. Using the self-consistent calculation above, we estimate the magnitude of the relaxation component due to $B^h\chi^h$ to be $(1/T_1)_{\rm NQR}=1.0T$ (sec^{-1}K^{-1}), less than one-fourth the value of Yasuoka *et al.* As a check of the Imai experimental result, we have measured the Cu(2) $(1/T_1)_{\rm NQR}$ from 100 to 500 K. Figure 15 shows our $(1/T_1)_{\rm NQR}$ data versus temperature. The data above 200 K appear to have a linear component with a slope steeper than our estimate; however, there is no way to be sure that there is not another temperature-dependent component also present in this temperature range. Note that $(1/T_1)_{\rm NQR}$ increases by 30% between 100 and 200 K due to some non-Korringa mechanism. This could be the contribution from the oxygen holes in the plane. Exploration of this possibility is beyond the scope of this paper.

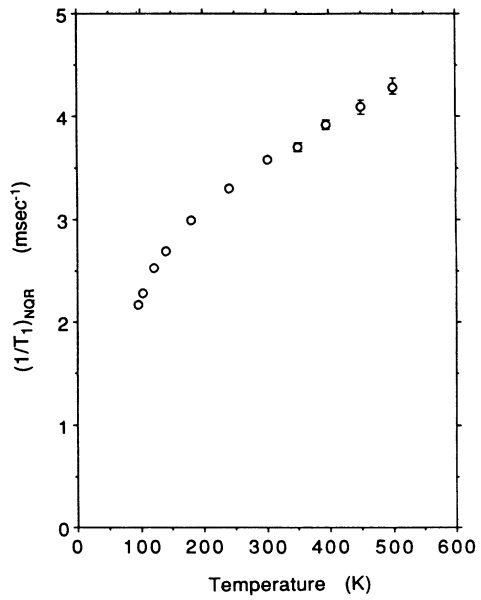

FIG. 15. $(1/T_1)_{\rm NQR}$ for the Cu(2) nuclei vs T. The relaxation rate seems to have a linear temperature dependence as pointed out by Yasuoka *et al.* (Ref. 30). We have extended the data to higher temperatures and we find that the linear term persists.

VIII. SUMMARY AND CONCLUSIONS

At this point, using the data reported in this paper and that reported previously, we can summarize our findings and viewpoint as follows. The symmetries and temperature dependences of the shifts, as discussed in the text, appear to rule out the planar state, and support the view that the spin contribution to the shift vanishes at 0 K.

Interpreting the shift at 0 K as being solely orbital in nature makes the orbital shifts at both Cu(1) and Cu(2) very similar in magnitude and anisotropy, with the Cu(1) axial about the a axis, the Cu(2) axial about the c axis, as expected. These data then fit in well with the electric-field-gradient data to support a model in which both Cu(1) and Cu(2) are close to Cu^{2+} with a single hole in the y^2-z^2 or x^2-y^2 orbits, respectively.

Assumption of only two numbers [typical values for the Cu(2) spin-orbit coupling λ and for the core-polarization parameter κ] is sufficient, when applied to experimental data (the measured $\langle S_z \rangle$ from neutron diffraction of $YBa_2Cu_3O_6$ in the antiferromagnetic state, our data on spin and orbital contributions to the shifts, and our measurement of the anisotropy of W_1 to enable us to calculate $\langle 1/r^3 \rangle$, the energies to the excited states, and the various hyperfine coupling constants. The resultant values fall right in the range expected theoretically for a Cu^{2+} having an electron spin of $\frac{1}{2}$ and a permanent electron-spin moment.

Since, as pointed out above, the chemical-shift and electric-field-gradient data strongly support the concept that the Cu(1) and Cu(2) atoms are very similar, we expect that if the Cu(2) has a permanent electron-spin moment, as it appears to, most likely the Cu(1) does as well.

The Cu(2) spin-lattice relaxation can be understood in terms of fluctuations of the hyperfine field arising from fluctuations of the orientations of the Cu(2) spin moments, but the physical origin of the correlation time τ_0 and of its temperature dependences in both normal and superconducting states is a matter of conjecture.

For the Cu(1), the spin contribution to the shift, the isotropy of the spin shift and of the spin-lattice relaxation rate, W_1, the temperature dependence of W_1, and the numerical size of the Korringa product $(K^S)^2T/W_1$ make it highly likely that the shift and spin-lattice relaxation arise from coupling of the Cu(1) nuclei to a conduction band (or Fermi liquid) of weakly interacting carriers via a transferred hyperfine coupling to the Cu(1) 4s wave function.

There appears to be no sign of the Cu(1) 3d hole electron spin in the angular dependence of either the Knight shift or W_1. We speculate that the spin must be scattered at very high rate, making the corresponding correlation time very short.

Below T_c, the Cu(1) Knight shift obeys a BCS spin-singlet, $l=0$ weak-coupling $[2\Delta(0)=3.52k_BT_c]$ Yosida function. It is therefore surprising that the Cu(1) W_1, does not appear to fit the corresponding BCS exponential temperature dependence at low temperatures, since both measurements essentially measure thermal excitations across the energy gap. As W_1 becomes smaller, however, one must keep in mind the possibility that another mechanism comes to dominate the relaxation.

Below T_c, the Cu(2) Knight-shift data can be fit with BCS strong-coupling expressions for spin singlet with either $l=0$ or 2 pairing. Our best data seem to favor the $l=0$ pairing state, but do not rule out the $l=2$ pairing state. In either case, the strong coupling is manifested both in the precipitous drop of χ^S just below T_c and in the large energy gap which is implied by the data.

The existence of two energy gaps, one at $3.5k_BT_c$, the other $5-6k_BT_c$ have been detected by Tsai[31] in tunneling experiments involving oriented films. These numbers seem to match the two gaps needed for our data, associated with the chain and plane portion of the Fermi surface. Warren *et al.*[19] also deduced two energy gaps of roughly these magnitudes from their early work on NQR spin-lattice relaxation.

Up to this point we have described the Cu(2) 3d hole as if it was local, permanent moment above T_c and part of a conduction band below T_c. This is the most straightforward way to describe the data in both regimes. However, it seems to us quite unreasonable to think that the Cu(2) could really have gone from a strong-correlation Hubbard limit to a weak-correlation Hubbard limit at 90 K. Rather, there must be something much subtler happening. We note that there is a similar situation in another problem, the Kondo effect. With respect to that problem, sometimes it was written that the magnetic atom "loses its moment" at low temperature. This is misleading because the Kondo problem is described by the same Hamiltonian, which assumes a permanent moment, at all temperatures. The proper description is that the coupling of the permanent moment to the conduction electrons cause its susceptibility to fall below its Curie law value at low temperatures.

In a similar way, we believe that it may be useful to consider how the Cu(2) permanent moment can take on, as far as spin polarization is concerned, the character of a (strong-coupling) conduction band described in the superconducting state by the generalized BCS theory.

Here it may be significant that the 1:2:3 materials of depleted oxygen, which are insulators, are antiferromagnets. The existence of charge carriers seems to prevent the antiferromagnetic transition from occurring in the 90-K material even though, as we know from NMR, there is still a strong Cu(2)-Cu(2) antiferromagnetic spin coupling in the normal state.[32] The suggestion that exchange coupling between planar holes and Cu(2) spins suppresses the antiferromagnetic coupling is well known. Moreover, as Hammel *et al.*[33] have shown, the planar O nuclei obey the conduction electron (Fermi liquid) law $T_1T=\text{const}$ in the normal state, lending support to the view of the planar holes in the normal state as being in a conduction band. Thus, if the Cu(2) Knight shift in the superconducting state suggests singlet-spin pairing, one naturally wonders whether the planar O holes are pairing, and whether, when paired, the O holes are as effective in preventing the Cu(2) antiferromagnetism as they are in the normal state. Thus, as the O spins pair, some form of Cu spin pairing expressing antiferromagnetism may be favored. Since the antiferromagnetic state of the O_6 material is fixed in space, but spin pairing of con-

duction electrons runs through space, one would be surprised to see a simple antiferromagnetic state appear for the 90-K material when there was spin pairing of O holes. However, there still might be some way that an antiferromagnetic benefit for the Cu(2)'s from pairing of O holes creates some form of Cu(2)-Cu(2) spin correlation.

No doubt the above speculations are crude and overly simplistic. We present them in the spirit, however that it seems remarkable that the Cu(2) which appears to be described so satisfactorily as possessing a permanent spin moment above T_c seems to take on the character of itinerant charge carrier below T_c at least as far as spin polarizability is concerned. One naturally wonders whether that resolution of this mystery lies close to the explanation of the mechanism of superconductivity.

ACKNOWLEDGMENTS

The authors take pleasure in acknowledging their fruitful collaboration and interchange of ideas with H. Monien and D. Pines, as well as the helpful interactions with R. Martin, S. Renn, J. Annett, and A. Leggett. This research was supported by the U.S. Department of Energy, Division of Materials Research, under Contract No. DE-AC02-76ER01198, and by the National Science Foundation Division of Materials Research under Contract No. DMR 87-14555.

---

*Also at Department of Chemistry.

[1]D. E. MacLaughlin, in *Solid State Physics,* edited by H. Ehrenreich, F. Seitz, and D. Turnbull (Academic, New York, 1976), Vol. 31; J. Winter, *Magnetic Resonance in Metals* (Clarendon, Oxford, 1971).

[2]A. J. Leggett, Rev. Mod. Phys. **47**, 331 (1975).

[3]J. T. Markert, T. W. Noh, S. E. Russek, and R. M. Cotts, Solid State Commun. **63**, 847 (1987).

[4]H. Alloul, P. Mendels, G. Collin, and P. Monod, Phys. Rev. Lett. **61**, 746 (1988).

[5]G. Balakrishnan, R. Dupree, I. Farnan, D. McK Paul, and M. E. Smith, J. Phys. C **21**, L847 (1988).

[6]H. Alloul, T. Ohno, and P. Mendels, Phys. Rev. Lett **63**, 1700 (1989).

[7]K. Yosida, Phys. Rev. **110**, 769 (1958).

[8]M. Takigawa, P. C. Hammel, R. H. Heffner, and Z. Fisk, Phys. Rev. B **39**, 7371 (1989).

[9]D. E. Farrell, B. S. Chandrasekhar, M. R. DeGuire, M. M. Fang, V. G. Kogan, J. R. Clem, and D. K. Finnemore, Phys. Rev. B **36**, 4025 (1987).

[10]C. H. Pennington, D. J. Durand, C. P. Slichter, J. P. Rice, E. D. Bukowski, and D. M. Ginsberg, Phys. Rev. B **39**, 2902 (1989).

[11]H. Y. Carr and E. M. Purcell, Phys. Rev. **94**, 630 (1954); S. Meiboom and D. Gill, Rev. Sci. Instrum. **29**, 688 (1958).

[12]Joseph H. Ross, Jr., Ph.D. thesis, University of Illinois at Urbana-Champaign, 1986 (unpublished).

[13]S. E. Shore, J.-Ph. Ansermet, C. P. Slichter, and J. H. Sinfelt, Phys. Rev. Lett. **58**, 953 (1987).

[14]M. Mali, D. Brinkmann, L. Pauli, J. Roos, H. Zimmermann, and J. Hulliger, Phys. Lett. A **124**, 112 (1987).

[15]H. Monien and D. Pines, following paper, Phys. Rev. B **41**, 6297 (1990).

[16]R. H. Hammond and G. M. Kelly, Phys. Rev. Lett. **18**, 156 (1967).

[17]F. Reif, Phys. Rev. **106**, 208 (1957).

[18]P. W. Anderson, Phys. Rev. **96**, 266 (1954).

[19]W. W. Warren, Jr., R. E. Walstedt, G. F. Brennert, G. P. Espinosa, and J. P. Remeika, Phys. Rev. Lett. **59**, 1860 (1987).

[20]C. P. Slichter, *Principles of Magnetic Resonance,* 2nd ed. (Springer, Berlin, 1980).

[21]T. Moriya, J. Phys. Soc. Jpn. **19**, 681 (1964).

[22]F. Mila, and T. M. Rice, Physica C **157**, 561 (1989).

[23]P. W. Anderson and P. Morel, Phys. Rev. **123**, 1911 (1961).

[24]H. Monien, D. Pines, and C. P. Slichter (unpublished).

[25]S. Massidda, J. Yu, A. J. Freeman, and D. D. Koelling, Phys. Lett. A **122**, 198 (1987).

[26]L. C. Hebel and C. P. Slichter, Phys. Rev. **113**, 1504 (1959); J. R. Clem, Ann. Phys. **40**, 268 (1966).

[27]B. Bleaney, K. D. Bowers, and M. H. L. Pryce, Proc. R. Soc. London, Ser. A **228**, 166 (1955).

[28]Y. Yamada, K. Ishida, Y. Kitaoka, K. Asayama, H. Takagi, H. Iwabuchi, and S. Uchida, J. Phys. Soc. Jpn. **57**, 2663 (1988); H. Yasuoka, T. Shimizu, Y. Veda, and K. Kosuge, *ibid*, **57**, 2659 (1988).

[29]A. Junod, A. Bezinge, and J. Muller, Physica C **152**, 50 (1988).

[30]H. Yasuoka, T. Imai, and T. Shimizu, in *Strong Correlations and Superconductivity,* edited by H. Fukuyama, S. Maekawa, and A. P. Malozemoff (Springer, Berlin, 1989).

[31]J. S. Tsai and I. Takeuchi, in *Strong Correlations and Superconductivity,* edited by H. Fukuyama, S. Maekawa, and A. P. Malozemoff (Springer, Berlin, 1989).

[32]C. H. Pennington, D. J. Durand, C. P. Slichter, J. P. Rice, E. D. Bukowski, and D. M. Ginsberg, Phys. Rev. B **39**, 274 (1989).

[33]P. C. Hammel, M. Takigawa, R. H. Heffner, Z. Fisk, and K. C. Ott, Phys. Rev. Lett. **63**, 1992 (1989).